Genomic instability and endoreduplication triggered by *RAD17* deletion

Xin Wang,[1] Lee Zou,[2,3] Huyong Zheng,[1] Qingyi Wei,[4] Stephen J. Elledge,[2,3,5] and Lei Li[1,6,7]

[1]Departments of Experimental Radiation Oncology, [4]Epidemiology, and [6]Molecular Genetics, University of Texas M.D. Anderson Cancer Center, Houston, Texas 77030; [2]Verna & Mars McLean Department of Biochemistry and Molecular Biology, [3]Howard Hughes Medical Institute, and [5]Department of Molecular and Human Genetics, Baylor College of Medicine, Houston, Texas 77030, USA

Cell cycle checkpoints are critical for genomic stability. Rad17, a component of the checkpoint clamp loader complex (Rad17/Rfc2-5), is required for the response to DNA damage and replication stress. To explore the role of Rad17 in the maintenance of genomic integrity, we established somatic conditional alleles of *RAD17* in human cells. We find that *RAD17* is not only important for the Atr-mediated checkpoint but is also essential for cell viability. Cells lacking *RAD17* exhibited acute chromosomal aberrations and underwent endoreduplication at a high rate. Therefore, *RAD17* links the checkpoint to ploidy control and is essential for the maintenance of chromosomal stability.

Supplemental material is available at http://www.genesdev.org.

Received December 6, 2002; revised version accepted February 19, 2003.

The DNA damage and replication checkpoint is essential for the maintenance of genomic stability. Recent studies have established a framework of the signal transduction process in mammalian cells (Zhou and Elledge 2000; Rouse and Jackson 2002). Two protein kinases of the PI-3-related protein family, Atm and Atr, are key components of the pathway. Both Atm and Atr are important for the maintenance of genomic stability. Atm is primarily involved in the response to double-strand DNA breaks (DSBs), whereas Atr responds to both DSBs and other damage causing replication stress (Abraham 2001). Current evidence suggests that Atr and Atm are signal-initiating kinases for the checkpoint kinase cascade that leads to activation of downstream targets including Brca1, Chk1, Chk2, p53, and Nbs1. How Atr or Atm is activated by DNA damage and how other components of the checkpoint are involved in the activation process, however, remains to be elucidated.

In fission yeast, activation of the *rad3*-dependent checkpoint requires Rad1, Rad9, Hus1, and Rad17 (Martinho et al. 1998). Rad1, Rad9, and Hus1 form a trimeric complex resembling the PCNA trimer that acts as a sliding clamp for DNA polymerases during DNA synthesis and interacts with proteins involved in cell-cycle control, DNA repair, and chromatin assembly (Kaur et al. 2001). The Rad17 protein is conserved with subunits of the replication factor C (RFC), which loads the PCNA clamp onto primed DNA structure. In human cells, Rad17 was found to be in a heteropentameric complex with RFC subunits. Meanwhile, Rad17 also interacts with the Rad1/Rad9/Hus1 trimer (Volkmer and Karnitz 1999; Caspari et al. 2000; Lindsey-Boltz et al. 2001). Therefore, a checkpoint sliding clamp-loader model for lesion recognition has been proposed (O'Connell et al. 2000; Venclovas and Thelen 2000). Rad3-mediated Rad26 phosphorylation, however, has been observed in fission yeast in the absence of the clamp-clamp loader proteins (Edwards et al. 1999). Similarly in budding yeast, the Atr/Atrip homolog, Mec1/Ddc2, and the checkpoint clamp and clamp loader complex (Rad17/Ddc1/Mec3-Rad24/Rfc2-5 in budding yeast) could both localize to the damage site independently (Kondo et al. 2001; Melo et al. 2001). These observations suggest that the clamp-loader complex may not be essential for damage recognition of the Mec1 or Rad3 kinases. More recent studies in humans suggest that Rad17 is required for loading the Rad1/Rad9/Hus1 clamp onto damaged DNA and may act to facilitate Atr-dependent phosphorylation of downstream targets (Zou et al. 2002). In this study, we have shown that the function of *RAD17* is critical in the Atr-dependent checkpoint signal initiation and is also important in the maintenance of genomic stability.

[*Keywords*: *RAD17*; DNA damage; checkpoint; endoreduplication]
[7]Corresponding author.
E-MAIL leili@mdanderson.org; FAX (713) 794-5369.
Article published online ahead of print. Article and publication date are at http://www.genesdev.org/cgi/doi/10.1101/gad.1065103.

Results and Discussion

Generation of RAD17 somatic conditional alleles

To investigate the function of the clamp-loader complex, we performed gene targeting in human HCT116 colon epithelial cells and constructed a conditional *RAD17*-null cell line (*RAD17*$^{flox/-}$), in which one allele of *RAD17* is disrupted by an in-frame insertion of the neomycin coding sequence, whereas the second allele has two lox sites flanking exon 5 (Fig. 1A,B). The amount of Rad17 in *RAD17*$^{flox/-}$ cells exhibited ~50% reduction before adenovirus-mediated Cre incision, indicating that the presence of lox sites flanking exon 5 in the conditioned allele has minimum effect on *RAD17* transcription or splicing. Upon adenovirus-mediated Cre incision, a decline in the amount of Rad17 could be detected within 2 d and the level of Rad17 became nearly undetectable by 4 d post infection, indicating a highly efficient removal of the conditional exon 5 in the *RAD17*$^{flox/-}$ mutant cells (Fig. 1C). As a control, cellular levels of the Rad9 protein were unaffected by Ad–Cre infection. However, loss of Rad17 severely inhibited damage-induced chromatin association of the Rad9 protein, which may be important for the recruitment of downstream targets (Zou et al. 2002; Supplemental Fig. 1).

RAD17 is essential for cell viability as assessed by clonogenic analysis. We found that >90% of Ad–Cre-infected *RAD17*$^{flox/-}$ cells were unable to form colonies, whereas *RAD17*$^{flox/+}$ cells (with one wild-type *RAD17*

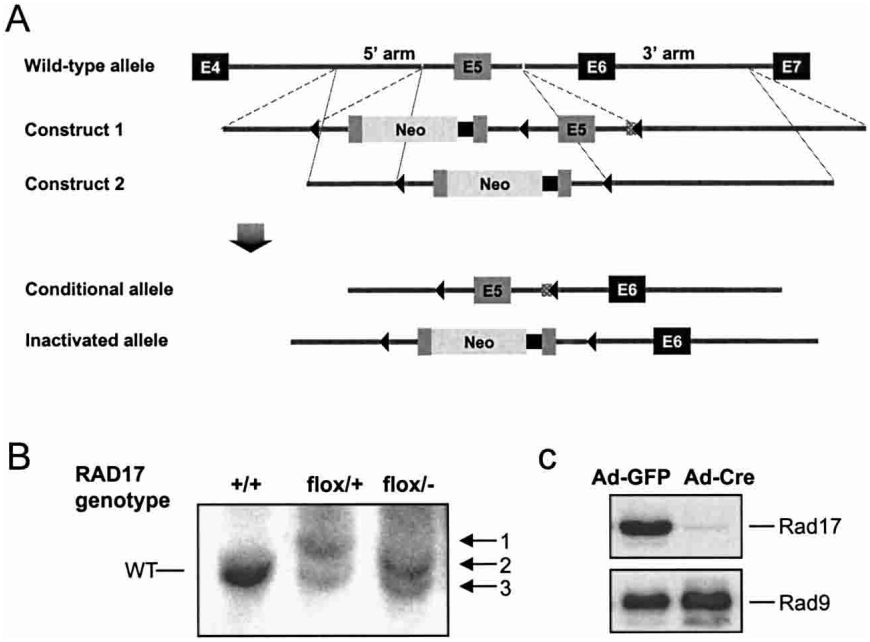

Figure 1. Generation of a conditional *RAD17* allele in human somatic cells. (*A*) Targeting strategy for establishing a conditional *RAD17* allele. Construct 1 contains a duplicated exon 5 as well as an exon 5 disrupted in-frame with the complete coding sequence of the neomycin resistance (Neo) gene and polyadenylation sequence (black squares). Three lox sites (triangles) were positioned as indicated. Following targeting with Construct 1, exon 5 with the Neo insertion was removed by selective Cre incision between the first two lox sites to generate the Conditional allele and allow recycle of the Neo marker. A second round of targeting with Construct 2 generated the Inactivated allele. (*B*) Southern blot analysis of genomic DNA isolated from the indicated cell lines after digestion with SpeI. +/+, *RAD17* wild-type HCT116 cells by the presence of wild-type alleles (8.1 kb); flox/+, cells that had been successfully targeted with Construct 1, showing a wild-type band and band 1 (9.6 kb); flox/–, cells with the Inactivated allele (band 3, 8.5 kb) and the Conditional allele (band 3, 7.3 kb). A SpeI site immediately downstream of the last lox site in both Construct 1 and 2 reduced the length of the conditional allele band (band 3) by 0.8 kb, compared with the wild-type band. (*C*) Immunoblot analysis of $RAD17^{flox/-}$ cells 3 d after Ad–Cre and Ad–GFP infection, respectively. The loss of the Rad17 protein was nearly complete whereas Rad9 levels remained constant in both cells.

allele) showed no difference compared with $RAD17^{+/+}$ cells, indicating that Rad17 is essential for sustained cell growth. However, the majority of $RAD17^{flox/-}$ cells remained viable 5 d after Ad–Cre infection, allowing further phenotypic analysis of the loss-of-function Rad17 mutant (Supplemental Fig. 2).

Loss of RAD17 function leads to checkpoint signaling defect

To study the role of Rad17 in Atm- and Atr-mediated checkpoint activation, we examined damage-induced phosphorylation of Atm and Atr kinase targets. In $RAD17^{+/+}$ cells, UV treatment induced Chk1 phosphorylation on Ser 345, whereas γ-radiation induced Thr 68 phosphorylation on Chk2 (Matsuoka et al. 2000; Abraham 2001). In two independently derived $RAD17^{flox/-}$ mutants, however, phospho-Ser 345 on Chk1 was drastically reduced (Fig. 2B), indicating that the clamp-loader complex is required for Atr-mediated Chk1 phosphorylation. In contrast, IR-induced Thr 68 phosphorylation of Chk2 was not affected by loss of Rad17 (Fig. 2C). Similarly, damage-induced phosphorylation of Smc1 and Nbs1, which both rely on Atm for activation (Lim et al. 2000; Zhao et al. 2000; Kim et al. 2002; Yazdi et al. 2002), appeared to be normal in the absence of Rad17 (Fig. 2D,E). Together, these results suggest that Atm activation is independent of the clamp–clamp-loader complex. Furthermore, we found that the Chk2 Thr 68 phosphorylation was significantly enhanced in response to UV irradiation, which normally induces a low level of Chk2 phosphorylation in wild-type cells. This result suggests that the defect in Atr signaling caused by loss of Rad17 may allow Atm to have a compensatory role in activating the Chk2 kinase on UV damage, as double-strand breaks resulting from DNA damage-induced stalled replication forks could provide an alternative route for activating the Atm kinase. Such a crossover in downstream substrate selection, observed in fission yeast (Martinho et al. 1998), may offer secondary or compensatory protection against genotoxic agents in case one DNA damage-sensing branch is compromised.

Damage-induced mitotic delay is defective in loss of RAD17 function mutant

We next examined the radiation-induced G2/M checkpoint in cells lacking Rad17. $RAD17^{+/+}$, $RAD17^{flox/-}$, and $ATR^{flox/-}$ cells were infected with Ad–Cre and subsequently exposed to γ-radiation. Entry into mitosis was measured by flow cytometry combined with phospho-histone H3 immunofluorescent staining (Fig. 3A,B). In $RAD17^{+/+}$ cells, mitotic entry was effectively delayed by radiation treatment. In $RAD17^{flox/-}$ cells, however, the mitotic population was significantly higher, indicating a defective G2/M checkpoint resulting from loss of Rad17. In addition to the erroneous entry into mitosis upon radiation, $RAD17^{flox/-}$ cells also retained a persistent G1/G0 population despite 16 h of nocodazole block (Fig. 3B). A higher percentage of G1/G0 cells was also observed in Ad–Cre-infected $RAD17^{flox/-}$ cells without γ-radiation. This result suggests that the majority of these cells were noncycling cells, presumably arising from accumulated chromosomal damage through loss of Rad17. In $ATR^{flox/-}$ cells similarly treated, emergence of a prominent G1/G0 population was not observed. We believe that the acute onset of chromosomal breakage in the Atr-null cells, as shown in the subsequent experiment, may more rapidly promote apoptotic cell death (Cortez et al. 2001) instead of accumulation of G1/G0 cells.

The radiation-resistant mitotic entry of $RAD17^{flox/-}$ cells was also independently assessed by microscopic laser-scanning cytometry using phospho-histone H3 staining (Fig. 3C). Consistent with the flow cytometry analy-

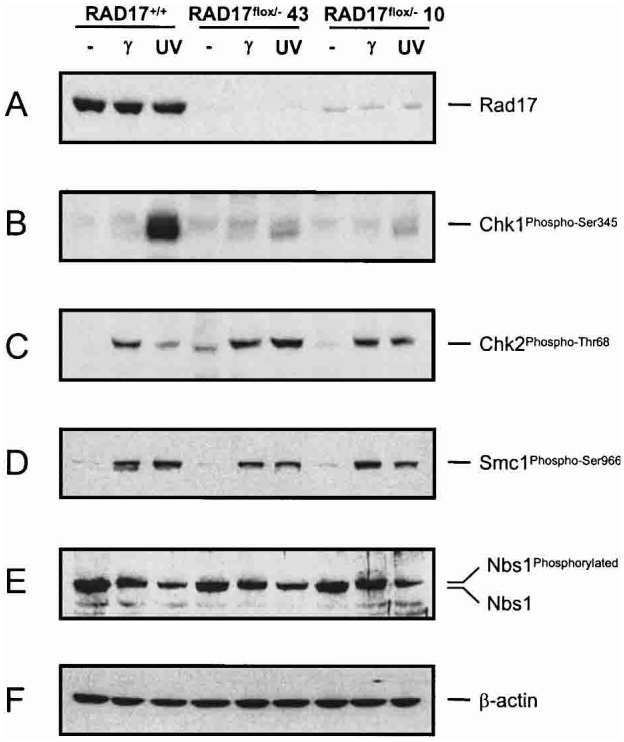

Figure 2. Defects in DNA damage-induced checkpoint activation in *RAD17*$^{flox/-}$ mutant cells. Wild-type (*RAD17*$^{+/+}$) and mutant (*RAD17*$^{flox/-}$) cells were exposed to γ-radiation (20 G) or UV (50 J/m^2) 3.5 d after Ad–Cre infection. Cells were harvested for protein extract preparation 2 h after treatment. The numbers 43 and 10 designate two independent *RAD17*$^{flox/-}$ clones—KO43 and KO10, respectively. (*A*) Rad17 levels in each mutant at the time of protein harvest. (*B*) Immunoblot with a phospho-Ser 345-specific Chk1 antibody. (*C*) Immunoblot analysis with a phospho-Thr 68-specific Chk2 antibody. (*D*) Immunoblot with a phospho-Ser 966-specific Smc1 antibody. (*E*) Immunoblot with an anti-Nbs1 antibody, showing unaltered Nbs1 phosphorylation pattern on DNA damage. (*F*) β-actin as loading control.

sis, IR treatment decreased mitotic fraction in *RAD17*$^{+/+}$ cells to <10% of the mock treated cells, whereas in *RAD17*$^{flox/-}$ and *ATR*$^{flox/-}$ cells, such reduction were 24.3% and 53.8%, respectively. Mitotic index analysis performed in parallel also generated similar results (Fig. 3D) in which loss of Rad17 enabled cells to enter mitosis in the presence of DNA damage. Collectively, these data again indicate an important role for Rad17 in DNA damage-induced mitotic delay.

Chromosomal instability and endoreduplication derived from RAD17 deletion

To assess the consequence of loss of Rad17 on chromosomal stability, we examined metaphase chromosome spreads 5 d after the conditioned *RAD17* allele was removed via Ad–Cre infection. In *RAD17*$^{+/+}$ cells infected with Ad–Cre, 1%–3% of metaphase chromosomes exhibited tetraploidy, whereas >97% were normal diploid (Fig. 4A). In the *RAD17*$^{flox/+}$ cells (with one wild-type *RAD17* allele), all 100 metaphase spreads examined were normal diploid (Fig. 4B). In *RAD17*$^{flox/-}$ cells (clone KO43), 75% of metaphase chromosomes showed structural aberrations including breaks, gaps, pulverized morphology, rings, dicentrics, and loss of chromosomes (Fig. 4C). Intriguingly, approximately half (58%) of the aberrant metaphase spreads also appeared to have undergone endoreduplication (rereplication; Fig. 4D), as indicated by the unresolved multiple chromatids structure. The

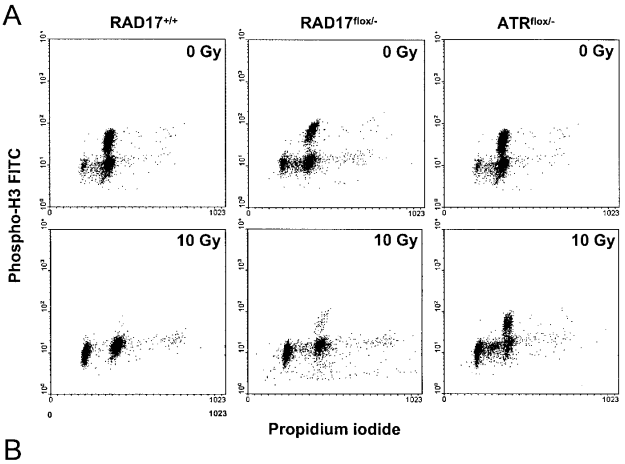

B

%	RAD17+/+	RAD17flox/-	ATRflox/-
G1/G0	15.31	33.95	13.45
S	3.68	4.3	3.43
G2	67	49	59.06
M	1.03	4.78	10.33

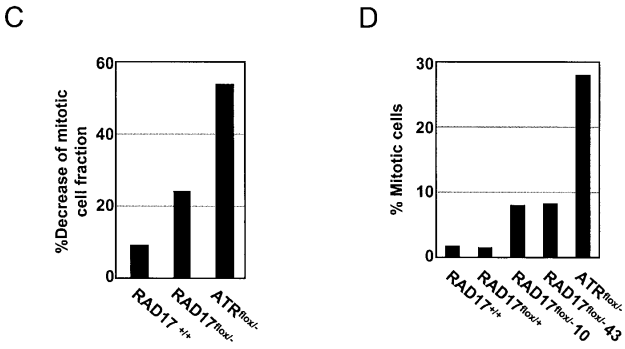

Figure 3. DNA damage-induced mitotic entry delay is impaired in *RAD17*$^{flox/-}$ mutant cells. (*A*) Mitotic entry checkpoint in *RAD17*$^{flox/-}$ cells. *RAD17*$^{+/+}$, *RAD17*$^{flox/-}$, and *ATR*$^{flox/-}$ cells were infected with Ad–Cre for 2.5 d and exposed to IR (10 G). Nocodazole (1 μg/mL) was added to the medium at the time of IR treatment to retain cells that have entered into mitosis. Sixteen hours later, cells were harvested for propidium iodide staining and immunostaining with an antibody to phospho-histone H3, a mitotic indicator, followed by FITC-conjugated secondary antibody. Flow cytometry was performed to determine DNA contents as well as the percentage of phospho-histone H3-positive cells. (*B*) Comparison of cell cycle distributions on DNA damage (10 Gy) in *RAD17*$^{+/+}$, *RAD17*$^{flox/-}$, and *ATR*$^{flox/-}$ cells. Cell cycle distribution was derived from flow cytometry analysis in *A*. The percentage of G2 cells was derived by subtracting the percentage of cells in mitosis from G2–M as determined by flow cytometry. (*C*) Samples prepared similarly as in *A* were analyzed by a laser scanning cytometer to determine phospho-histone H3-positive cells. Decrease in the mitotic cell fraction, induced by IR treatment, was expressed by the ratio of phospho-histone H3-positive cells between IR-treated and mock treated cells with each genotype. At least 5000 cells were scanned from each sample slide. (*D*) Mitotic index analysis by Giemsa staining after the indicated cells were treated with γ-radiation (10 G). Mitotic population is indicated as a percentage of total cell number. Each experiment was performed multiple times and representative results are shown.

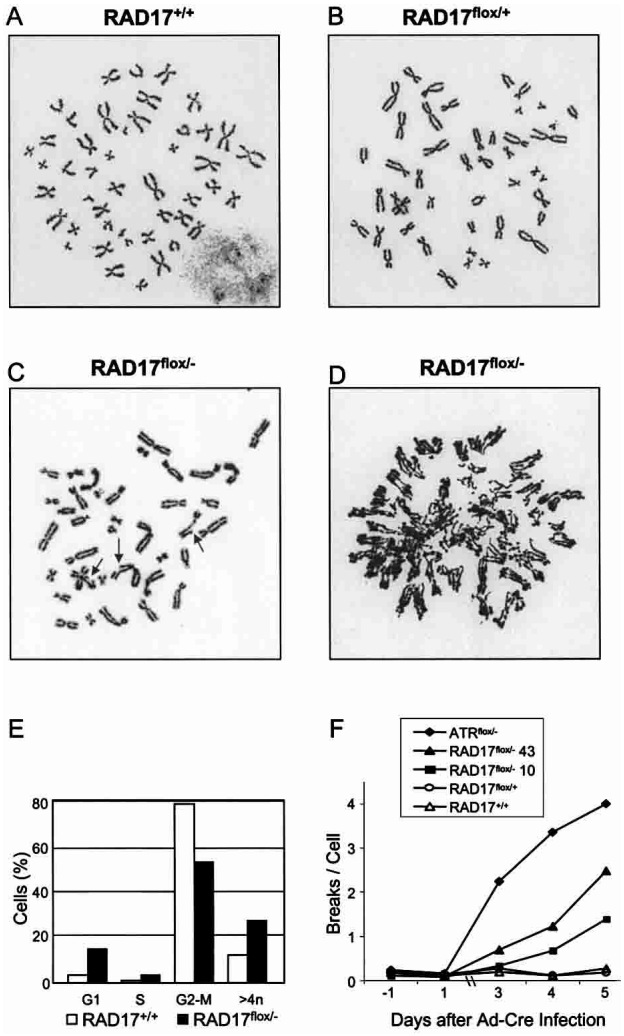

Figure 4. Chromosomal aberrations in *RAD17*$^{flox/-}$ cells. Metaphase chromosome spread of cells with indicated genotype 5 d after Ad–Cre infection. (*A*) Normal diploid metaphase spread found in *RAD17*$^{+/+}$ cells. (*B*) Normal diploid metaphase spread found in *RAD17*$^{flox/+}$ cells. (*C*) Chromosomal abnormalities in *RAD17*$^{flox/-}$ cells. Arrows point to gapped or broken chromosomes. (*D*) Metaphase chromosome spread from *RAD17*$^{flox/-}$ cells with partially endoreduplicated chromosomes. (*E*) Flow cytometry analysis of *RAD17*$^{+/+}$ and *RAD17*$^{flox/-}$ cells. Cells were infected with Ad–Cre for 3 d and subsequently subjected to 48 h of nocodazole block (200 ng/mL). The DNA contents of cells were determined by propidium iodide staining. The percentage of cells with hyperdiploid DNA content in the *RAD17*$^{flox/-}$ mutant was consistently higher than that of the *RAD17*$^{+/+}$ cells. (*F*) Accumulation of chromosome breaks in *RAD17* and *ATR* mutants. Cells with indicated genotypes were infected by Ad–Cre (day 0) and metaphase chromosome spreads were prepared at 3, 4, and 5 d post infection. Breaks per cell were derived from analysis of 100 metaphase spreads for each sample point.

degree of endoreduplication ranged from partial to nearly complete (Supplemental Fig. 3). Subsequent experiments were performed to ensure that the observed chromosomal abnormality was not caused by a secondary unrelated mutation or clonal variations. Analysis of another independent *RAD17*$^{flox/-}$ mutant (clone KO10) also showed similar chromosomal abnormalities, including endoreduplication. The progressiveness of the chromosomal aberrations was also observed. *RAD17*$^{flox/-}$ cells analyzed 3 d after Ad–Cre infection showed aberrant chromosomal structures in ~40% of the metaphase spread, but again, half of these exhibited partial or complete endoreduplication. Meanwhile, the early cell death of the Atr mutant (day 3) precludes the examination of endoreduplication at the time (day 5) when endoreduplication was primarily observed in the *RAD17* mutant.

To confirm the cytogenetics observation of endoreduplication, we analyzed the DNA content of the *RAD17*$^{flox/-}$ cells by flow cytometry. *RAD17*$^{+/+}$ and *RAD17*$^{flox/-}$ cells were infected with Ad–Cre for 3 d and cultured for an additional 2 d in the presence of nocodazole. The addition of nocodazole (200 ng/mL) blocked the onset of mitosis and allowed accumulation of cells with endoreduplicated DNA contents. Consistent with the observations in metaphase chromosome spreads, 27% of *RAD17*$^{flox/-}$ cells displayed greater than 4N DNA contents 4 d after Ad–Cre infection. In contrast, *RAD17*$^{+/+}$ cells had 12% cells with greater than 4N DNA contents (Fig. 4E). Moreover, the emergence of cells with greater than 4N DNA content could not be suppressed by nocodazole treatment, suggesting that mis-segregation during mitosis was not responsible for cells with increased DNA content. It should be noted that the value of 12% hyperdiploid cells in the wild-type samples as measured by FACS is misleading. To account for increases in cell size of *RAD17* mutant cells during the course of this experiment, we used a wide gating parameter that allowed the inclusion of a small number of two-cell aggregates that artificially increased the apparent number of hyperdiploid cells. When actual chromosome numbers were counted, <0.5% hyperdiploid cells were detected in cells containing a wild-type *RAD17* allele. Taken together, these observations seem to suggest a role of *RAD17* in replication control. One possibility could be that loss of *RAD17* allows replication licensing and results in re-firing of origins during the G2 phase before the intervening mitosis (Blow and Hodgson 2002).

We also investigated the accumulative effect of loss of Rad17 and Atr on chromosomal stability. Cells with the indicated genotypes were subjected to Ad–Cre infection and chromosomal breakage was analyzed for three consecutive days after infection. As shown in Figure 4F, loss of either Rad17 or Atr resulted in dramatic increase in chromosomal breakage and the number of breaks per cell accumulated with time. This result implicates frequent internal DNA damage, some of which presumably arises from replication disruption in proliferating cells, reflected by the acute onset and high frequency of chromosomal abnormalities on loss of Rad17 and Atr.

Our results indicate that *RAD17* is critical for Atr-dependent checkpoint signaling but is dispensable for damage-induced Atm activation. Therefore, the role of the clamp-loader complex may be to specifically facilitate Atr's function at the site of DNA damage. More interestingly, loss of Rad17 leads to DNA endoreduplication in a significant portion of the mutant cells as our cytogenetics data demonstrate that regions of chromosomes were rereplicated in *RAD17*$^{flox/-}$ cells. Furthermore, nocodazole treatment failed to prevent *RAD17*$^{flox/-}$ mutant from producing cells with hyperdiploid DNA content, ruling out the possibility that the rereplicated chromosomes are resulted from mis-segregation during mitosis. Therefore, these observations suggest a link between the Atr–Rad17 pathway and the replication licensing process in human cells. Such a link

may provide a novel mechanism on how gross chromosomal aberrations can arrive through a disrupted checkpoint.

Notably, the severity of phenotypes in *RAD17*$^{flox/-}$ cells is less profound than that of the isogenic *ATR*$^{flox/-}$ cells. *RAD17*$^{flox/-}$ cells survive significantly longer than *ATR*$^{flox/-}$ cells and exhibited little apoptotic population (Cortez et al. 2001). Defect in damage-induced mitotic delay appears to be less severe in *RAD17*$^{flox/-}$ cells compared with *ATR*$^{flox/-}$ cells. Moreover, accumulation of chromosomal damage is accelerated in *ATR*$^{flox/-}$ cells relative to *RAD17*$^{flox/-}$ cells. These observations suggest that Atr might carry out some of its functions in a Rad17-independent manner and consequently limited the severity of *RAD17*$^{flox/-}$ phenotypes. In fission yeast, a low level of HU-induced Cds1 kinase activity was observed in *rad17*-null mutant (Martinho et al. 1998). Additionally, double deletion of *rad3* and *rqh1*, a fission yeast homolog of the Blooms helicase, constitutes synthetic lethality whereas *rad17*/*rqh1* double deletion is viable, which suggest Rad17-independent function of the Rad3 kinase (Murray et al. 1997; Edwards et al. 1999). These findings seem to be consistent with the notion that Atr may provide some protection in the *RAD17* mutants. It is also important to note that these phenotypic distinctions could still be affected by residual amounts of Rad17 present in these cells, despite the fact that both mutants exhibited nearly complete target protein removal with similar kinetics.

Our results have uncovered a link between the Rad17-mediated checkpoint and the ploidy control in human cells. Notably, significant portions of the chromosomes were rereplicated in the *RAD17* mutant cells, indicating that these cells did not just replicate promiscuously, but instead, they had initiated a new round of DNA synthesis before mitosis. In fission yeast, reinitiation of DNA replication from fired origins is inhibited mainly by the B-type cyclin/CDKs associating with these origins (Wuarin et al. 2002). In contrast, vertebrate cells use multiple mechanisms, including cyclin/CDKs and geminin (Wohlschlegel et al. 2000; Tada et al. 2001; Coverley et al. 2002) to prevent reinitiation of DNA replication. Like the B-type cyclin/CDK in fission yeast, *Xenopus* Atr and Rad9 are also recruited onto chromatin during the initiation of DNA replication (You et al. 2002). It is possible that Atr and Rad17 may associate with fired origins and function in conjunction with the cyclin/CDKs to prevent reinitiation. Alternatively, the Atr–Rad17 pathway may generate a signal of ongoing replication that interferes with the licensing of origins. It is also possible that the ATR–Rad17 pathway might prevent rereplication through a more indirect mechanism.

Our findings provide direct evidence that the *RAD17* gene has a crucial role in the maintenance of chromosomal stability. Cells lacking the *RAD17* gene not only accumulate DSBs but also rereplicate their chromosomes, underscoring the importance of Rad17 in preventing chromosomal aberrations frequently displayed by cancer cells. Specific alleles of *RAD17* may yield viable separation of function mutants and promote tumorgenesis despite the fact that complete loss of Rad17 leads to cell death. Our group and others have shown that Rad17 exhibits damage-induced phosphorylation on Ser 635 and Ser 645 in an Atm/Atr-dependent manner (Bao et al. 2001; Wang et al. 2001; Zou et al. 2002). A Rad17 mutant bearing Ala substitutions on both serines, however, was able to rescue the cell lethality of the *RAD17*$^{flox/-}$ mutant (X. Wang and L. Li, unpubl.). Such mutations are likely candidates for *RAD17* tumorgenic alleles.

Material and methods

Cell lines and antibodies

The human colon epithelial HCT116 cell line used for the generation of *RAD17* mutants was obtained from ATCC. The Atr$^{flox/-}$ cell lines has be been described previously (Cortez et al. 2001). All cells were maintained in DMEM plus 10% FCS. The polyclonal antibodies against phospho-Chk1 (Ser 345) and phospho-Chk2 (Thr 68) were products of Cell Signalling Technology. The monoclonal antibody against Chk1 was purchased from Santa Cruz Technology. Rabbit antibody against Rad17 was raised against a recombinant protein containing Leu 311 to Ala 614 (Wang et al. 2001). Antibody against Nbs1 was obtained from Novus Biologicals. Phospho-Ser 966 Smc1 antibody was a kind gift from Jun Qin (Baylor College of Medicine, Houston, TX). Ad–Cre was produced by the Gene Therapy Center (Baylor College of Medicine, Houston, TX). Ad–GFP–Cre was a kind gift from Jeffrey Rosen (Baylor College of Medicine, Houston, TX). Where indicated, Cells were irradiated with a Nasatron ^{137}Cs source at a dose rate of 4.3 Gy/min at room temperature. UV irradiation was delivered from a (254-nm) germicidal light.

Homologous targeting

Exon 5 was selected for targeting because the first coding exon (exon 2) is at a close proximity to the promoter region (<0.7 kb), prohibiting the promoter-trapping design strategy essential for somatic cellular targeting. Exons 3 and 4 are not frame-interrupting exons. Therefore, exon 5 (158 bp), a frame-interrupting exon, was chosen to establish the conditional allele. Deletion of exon 5 will effectively eliminate Gly 118 through Thr 670 of Rad17 on Cre-mediated deletion. To ensure that the *neo* gene is still functional as a fusion protein, the exact fusion (Rad17 Met 1–Gln 117 upstream and in-frame with Neo-coding sequence) that would be produced in the targeted allele was tested and found to exhibit sufficient Neo activity for G418 selection.

After transfection with Construct 1, 960 Neo-resistant colonies were screened by Southern blot. Two clones, 17B12 and 17G36, were found to be correctly targeted judging from both 5′ and 3′ probes located outside the homologous arms. Before targeting the second *RAD17* allele, karyotyping analysis and cell-cycle damage response of both heterozygous mutants were analyzed and compared with the parental HCT116 cells and no haploinsufficiency was observed. Subsequently, the 17B12 mutant was subjected to partial Cre-mediated incision to remove the Neo-inserted exon 5. Both Southern blot and PCR analysis were performed to ensure the precise removal of the Neo-inserted exon 5. The resulting cell line, carrying a conditioned exon 5, was targeted with Construct 2 to inactivate the remaining wild-type allele. Two independent clones, KO10 and KO43, were found correctly targeted among 576 Neo-resistant colonies. Western blot was performed to determine if any truncated forms of Rad17 could be expressed from the disrupted alleles. A polyclonal antibody against the C-terminal half of Rad17 (Leu 311–Ala 614) detected no truncated forms of Rad17 in all the mutant cell lines used in this study.

Cell cycle analysis

Cells were harvested by trypsinization, fixed with ice-cold 70% ethanol. The DNA content is analyzed by standard flow cytometry procedures using propidium iodide (PI) staining. For immunofluorescent detection of phospho-histone H3, fixed cells were resuspended in 0.25% Triton X-100 in PBS and incubated on ice for 15 min and then incubated at room temperature for 3 h in PBS containing 1% BSA and 100 μg/mL of a mouse anti-phospho-histone H3 antibody (Sigma). Secondary staining was carried out with PBS containing 1% BSA and FITC-conjugated goat anti-mouse antibody (Jackson ImmunoResearch Laboratories) diluted at a ratio of 1:50. After a 30-min incubation at room temperature in the dark, cells were stained with PI and cellular fluorescence was measured by a FACScan flow cytometer. Each flow sample produced no less than 9000 gated events. Alternatively, the DNA content and fluorescence were measured by a laser scanning cytometer (CompuCyte, Inc.), in which

case no less than 5000 cells were scanned from each sample. Mitotic index was determined by counting mitotic cells after Giemsa staining.

Cytogenetic analysis

Colcemid (20 ng/mL) was added to cell culture 2 h before harvesting by trypsinization. Cells were then swollen for 10 min at 37°C in 0.075M KCl, and fixed for 20 min in methanol: acetic acid (3:1; vol:vol). Fixed cells were spotted onto microscopic slides and stained by 4% Giemsa in 0.01 M phosphate buffer (pH 6.8). For each sample, chromosomal breakage in 100 or 200 well-spread metaphase was counted. To ensure the accuracy of chromosome break scoring, blind samples were also independently analyzed by the cytogenetics core facility (MDACC).

Acknowledgments

We thank Jeff Rosen for providing an Ad–GFP–Cre virus, T. Lu, L. Wang, and the MDACC Cytogenetics Core for providing technical assistance, and David Cortez for helpful discussions. L.Z. is a fellow of the Cancer Research Fund of the Damon Runyon-Walter Winchell Foundation. S.J.E. is an investigator with the Howard Hughes Medical Institute and a Welch professor of biochemistry. This work is also supported by National Institutes of Health grants CA76172 (L.L.), CA91029 (L.L.), and GM44664 (S.J.E.).

The publication costs of this article were defrayed in part by payment of page charges. This article must therefore be hereby marked "advertisement" in accordance with 18 USC section 1734 solely to indicate this fact.

References

Abraham, R.T. 2001. Cell cycle checkpoint signaling through the ATM and *ATR* kinases. *Genes & Dev.* **15:** 2177–2196.

Bao, S., Tibbetts, R.S., Brumbaugh, K.M., Fang, Y., Richardson, A., Ali, A., Chen, S.C., Abraham, R.T., and Wang, X.F. 2001. *ATR*/ATM-mediated phosphorylation of human Rad17 is required for genotoxic stress responses. *Nature* **411:** 969–974.

Blow, J.J. and Hodgson, B. 2002. Replication licensing—defining the proliferative state? *Trends Cell. Biol.* **12:** 72–78.

Caspari, T., Dahlen, M., Kanter-Smoler, G., Lindsay, H.D., Hofmann, K., Papadimitriou, K., Sunnerhagen, P., and Carr, A.M. 2000. Characterization of Schizosaccharomyces pombe Hus1: A PCNA-related protein that associates with Rad1 and Rad9. *Mol. Cell. Biol.* **20:** 1254–1262.

Cortez, D., Guntuku, S., Qin, J., and Elledge, S.J. 2001. *ATR* and ATRIP: Partners in checkpoint signaling. *Science* **294:** 1713–1716.

Coverley, D., Laman, H., and Laskey, R.A. 2002. Distinct roles for cyclins E and A during DNA replication complex assembly and activation. *Nat. Cell. Biol.* **4:** 523–528.

Edwards, R.J., Bentley, N.J., and Carr, A.M. 1999. A Rad3–Rad26 complex responds to DNA damage independently of other checkpoint proteins. *Nat. Cell. Biol* **1:** 393–398.

Kaur, R., Kostrub, C.F., and Enoch, T. 2001. Structure-function analysis of fission yeast Hus1–Rad1–Rad9 checkpoint complex. *Mol. Biol. Cell* **12:** 3744–3758.

Kim, S.T., Xu, B., and Kastan, M.B. 2002. Involvement of the cohesin protein, Smc1, in Atm-dependent and independent responses to DNA damage. *Genes & Dev.* **16:** 560–570.

Kondo, T., Wakayama, T., Naiki, T., Matsumoto, K., and Sugimoto, K. 2001. Recruitment of Mec1 and Dcd1 checkpoint proteins to double-strand breaks through distinct mechanisms. *Science* **294:** 867–870.

Lim, D.S., Kim, S.T., Xu, B., Maser, R.S., Lin, J., Petrini, J.H., and Kastan, M.B. 2000. ATM phosphorylates p95/nbs1 in an S-phase checkpoint pathway. *Nature* **404:** 613–617.

Lindsey-Boltz, L.A., Bermudez, V.P., Hurwitz, J., and Sancar, A. 2001. Purification and characterization of human DNA damage checkpoint Rad complexes. *Proc. Natl. Acad. Sci.* **98:** 11236–11241.

Martinho, R.G., Lindsay, H.D., Flaggs, G., DeMaggio, A.J., Hoekstra, M.F., Carr, A.M., and Bentley, N.J. 1998. Analysis of Rad3 and Chk1 protein kinases defines different checkpoint responses. *EMBO J.* **17:** 7239–7249.

Matsuoka, S., Rotman, G., Ogawa, A., Shiloh, Y., Tamai, K., and Elledge, S.J. 2000. Ataxia telangiectasia-mutated phosphorylates Chk2 in vivo and in vitro. *Proc. Natl. Acad. Sci.* **97:** 10389–10394.

Melo, J.A., Cohen, J., and Toczyski, D.P. 2001. Two checkpoint complexes are independently recruited to sites of DNA damage in vivo. *Genes & Dev.* **15:** 2809–2821.

Murray, J.M., Lindsay, H.D., Munday, C.A., and Carr, A.M. 1997. Role of Schizosaccharomyces pombe RecQ homolog, recombination, and checkpoint genes in UV damage tolerance. *Mol. Cell. Biol.* **17:** 6868–6875.

O'Connell, M.J., Walworth, N.C., and Carr, A.M. 2000. The G2-phase DNA-damage checkpoint. *Trends Cell. Biol.* **10:** 296–303.

Rouse, J. and Jackson, S.P. 2002. Interfaces between the detection, signaling, and repair of DNA damage. *Science* **297:** 547–551.

Tada, S., Li, A., Maiorano, D., Mechali, M., and Blow, J.J. 2001. Repression of origin assembly in metaphase depends on inhibition of RLF-B/Cdt1 by geminin [see Comments]. *Nat. Cell. Biol.* **3:** 107–113.

Venclovas, C. and Thelen, M.P. 2000. Structure-based predictions of Rad1, Rad9, Hus1 and Rad17 participation in sliding clamp and clamp-loading complexes. *Nucleic Acids Res.* **28:** 2481–2493.

Volkmer, E. and Karnitz, L.M. 1999. Human homologs of Schizosaccharomyces pombe rad1, hus1, and rad9 form a DNA damage-responsive protein complex. *J. Biol. Chem.* **274:** 567–570.

Wang, X., Wang, L., Callister, M.D., Putnam, J.B., Mao, L., and Li, L. 2001. Human Rad17 is phosphorylated upon DNA damage and also overexpressed in primary non-small cell lung cancer tissues. *Cancer Res.* **61:** 7417–7421.

Wohlschlegel, J.A., Dwyer, B.T., Dhar, S.K., Cvetic, C., Walter, J.C., and Dutta, A. 2000. Inhibition of eukaryotic DNA replication by geminin binding to Cdt1. *Science* **290:** 2309–2312.

Wuarin, J., Buck, V., Nurse, P., and Millar, J.B. 2002. Stable Association of mitotic cyclin B/Cdc2 to replication origins prevents endoreduplication. *Cell* **111:** 419–431.

Yazdi, P.T., Wang, Y., Zhao, S., Patel, N., Lee, E.Y., and Qin, J. 2002. SMC1 is a downstream effector in the ATM/NBS1 branch of the human S-phase checkpoint. *Genes & Dev.* **16:** 571–582.

You, Z., Kong, L., and Newport, J. 2002. The role of single-stranded DNA and polymerase alpha in establishing the *ATR*, Hus1 DNA replication checkpoint. *J. Biol. Chem.* **277:** 27088–27093.

Zhao, S., Weng, Y.C., Yuan, S.S., Lin, Y.T., Hsu, H.C., Lin, S.C., Gerbino, E., Song, M.H., Zdzienicka, M.Z., Gatti, R.A., et al. 2000. Functional link between ataxia-telangiectasia and Nijmegen breakage syndrome gene products. *Nature* **405:** 473–477.

Zhou, B.B. and Elledge, S.J. 2000. The DNA damage response: Putting checkpoints in perspective. *Nature* **408:** 433–439.

Zou, L., Cortez, D., and Elledge, S.J. 2002. Regulation of *ATR* substrate selection by Rad17-dependent loading of Rad9 complexes onto chromatin. *Genes & Dev.* **16:** 198–208.